

VISWANATH G. AKKILI<sup>1†</sup>, HANSUNG LEE<sup>2†</sup>, SUHYEON KIM<sup>1</sup>, JUN-HUI CHOI<sup>2,3</sup>,  
CHOONG-HEUI CHUNG<sup>1</sup>, JOON SIK PARK<sup>1</sup>, JAE-HYUN LEE<sup>2,3</sup>, BYUNGMIN AHN<sup>2,3</sup>,  
YOON-KEE KIM<sup>1\*</sup>, SANGYEOP LEE<sup>1\*</sup>

## INFLUENCE OF MULTILAYER STRUCTURE ON THE STRUCTURAL AND MECHANICAL PROPERTIES OF TiAlN/CrN COATINGS FOR ADVANCED MACHINING APPLICATIONS

This study investigates single and multilayer TiAlN/CrN nanocomposite thin films developed using an RF magnetron sputtering system. The TiAlN and CrN layers showed a high degree of orientation, with the (200) peak being the strongest peak in both layers, and a multilayer structure was clearly observed. The surface roughness analysis using atomic force microscopy (AFM) and cross-sectional transmission electron microscopy (TEM) revealed that the TiAlN/CrN coatings had a smoother surface than the single-layer coatings and minimal intermixing between the two layers. Depth-sensing indentation measurements were used to measure the hardness and Young's modulus of the coatings, demonstrating that TiAlN/CrN coating had the highest hardness (~16.38 GPa) and elastic modulus (~3.82 GPa) among all the coatings studied. This indicates that the TiAlN/CrN multilayer coating possesses superior mechanical properties due to its interface strength. Our findings suggest that these multilayer coatings have potential applications in tribological and decorative coatings.

*Keywords:* Metal nitrides; Multilayer coatings; RF magnetron sputtering; Nanoindentation; Interface control phenomena

### 1. Introduction

Transition metal nitride-based coatings are widely used in various applications due to their unique properties, including decorative and corrosion-resistant coatings for tribological applications [1]. Combining different materials, in particular, nitride materials with a few nanometers-thick layers in the form of multilayers, can produce coatings with superior properties compared to single-layer coatings in terms of enhanced hardness, better toughness, wear resistance, and oxidation resistance. These multilayers have been used to create a variety of nitride coatings, such as TiN/TiAlN [2], TiN/NbN [3], AlN/VN [4], and TiAlN/CrN [5]. The improved properties of these multilayer coatings can be attributed to several mechanisms, including Hall–Petch strengthening, the super modulus effect, dislocation blocking by layer interfaces, and strain effects at interfaces [6].

Titanium nitride (TiN) was one of the first coatings to be widely used for cutting tools due to its high hardness and wear resistance. However, TiN has limited oxidation resistance and thermal stability, which can be a problem in high-temperature

environments [7]. To overcome these limitations, titanium aluminium nitride (TiAlN) coatings were developed. These coatings have superior hardness, oxidation resistance, and thermal stability compared to TiN, making them a better choice for cutting tools and other applications. Despite the improved performance of TiAlN coatings, there is still a need for further improvements, particularly in the face of high temperatures and wear. One way to achieve this is by using multilayers of TiAlN combined with other nitride compounds. Chromium nitride (CrN) shows excellent corrosion and wear resistance. CrN added to TiAlN coatings causes an increase in their oxidation resistance [8]. The TiAlN/CrN system has been shown to have excellent wear resistance, making it a promising candidate for advanced machining applications [9].

The surface roughness and hardness are important parameters that can affect the performance of coatings in various applications. Several reports in the literature have demonstrated that these properties can vary depending on the deposition conditions and multilayer structure. In the study by Barshilia et al. [10], the TiAlN/CrN multilayer film was found to have a surface roughness of 4.4 nm and a hardness of 38 GPa. Baojian et al. [11],

<sup>1</sup> HANBAT NATIONAL UNIVERSITY, DEPARTMENT OF MATERIALS SCIENCE AND ENGINEERING, DAEJEON, 34158, KOREA

<sup>2</sup> AJOU UNIVERSITY, DEPARTMENT OF ENERGY SYSTEMS RESEARCH, SUWON, 16499, KOREA

<sup>3</sup> AJOU UNIVERSITY, DEPARTMENT OF MATERIALS SCIENCE AND ENGINEERING, SUWON, 16499, KOREA

<sup>†</sup> These authors contributed equally to this work

\* Corresponding authors: [sangyeob@hanbat.ac.kr](mailto:sangyeob@hanbat.ac.kr), [ykkim@hanbat.ac.kr](mailto:ykkim@hanbat.ac.kr)



reported that the maximum hardness of the untreated TiAlN/CrN coating was 25 GPa, but it increased to 36 GPa after Nb implantation. TiAlN/CrN coatings deposited by cathodic arc evaporation had a hardness of 26 GPa [12]. Ibrahim et al. [13], investigated the performance of TiAlN and TiAlN/CrN physical vapor deposition (PVD) coatings in resisting fretting fatigue failure of AISI P20 steel and found that the surface roughness and hardness of TiAlN were 16 nm and 23 GPa, respectively, while the corresponding values for TiAlN/CrN were 17 nm and 30 GPa. M. Panjan et al. [14], prepared multilayer coatings with varying bilayer periods using magnetron sputtering and found that the coatings had a columnar structure in both thin and thick layers, with strong interfaces and no intermixing. The TiAlN and CrN layers had the B1 NaCl-type crystal structure, and no other phases were observed.

In this article, we prepared single and multi-layered nanocomposite thin films using the RF magnetron sputtering technique to further investigate the structural and mechanical properties of these coatings and provide a comprehensive understanding of their potential applications.

## 2. Experimental details

### 2.1. Deposition details

The TiAlN, CrN, and TiAlN/CrN coatings were deposited on Si (100) substrates using a RF magnetron sputtering system. The substrates were cleaned using an ultrasonic bath in acetone, isopropyl alcohol and DI water for 5 minutes each and dried with nitrogen gas before being placed in the deposition chamber. The high-purity TiAl (99.99%) and Cr (99.95%) target materials were sputtered using Ar and N<sub>2</sub> gas as the sputtering gas at a pressure of 4 mTorr. The schematic diagram of the deposition system is shown in Fig. 1. To ensure uniform deposition, the substrate

holder was rotated during sputtering. This helped to improve the structural and mechanical properties of the coatings and reduce the formation of defects and voids. The deposition was carried out at a substrate temperature of 300°C with a constant RF power of 100 W for TiAlN and 150 W for CrN. The multilayer films were then deposited by alternating the deposition of TiAlN and CrN layers with a bilayer period of 20 nm. The thickness of each layer was controlled by the deposition time, with a total thickness of the multilayer film ranging from 20 to 22 nm.

### 2.2. Characterization of coatings

To characterize the coatings, X-ray diffraction (XRD), TEM, AFM, and nanoindentation measurements were used to investigate their structural, morphological, and mechanical properties. XRD measurements were performed to investigate the crystal structure and phase composition of the coatings, with the XRD patterns collected using a Rigaku SmartLab diffractometer with Cu K $\alpha$  radiation at a scan rate of 0.02°/s in the 2 $\theta$  range of 10-70°. TEM was used to study the interface characteristics of the multilayer films, with samples examined using a FEI Technai TEM, operated at 200 kV and equipped with a high-angle annular dark field (HAADF) detector and energy dispersive spectroscopy (EDS) system. The surface roughness and texture of the coatings were measured using AFM in tapping mode with an MFP-3D Origin, Asylum Research atomic force microscope. The mechanical properties of the layers were evaluated using a nanoindentation test with a Anton Paar High-precision surface mechanical analyzer. The hardness and elastic modulus were measured with a load range of 0.01-0.2 mN and a dwell time of 10 s. The measurements were performed at a temperature of 25°C with a loading rate of 0.01 mN/s. The indentation data were analyzed using the Oliver-Pharr method to obtain the hardness and elastic modulus values.

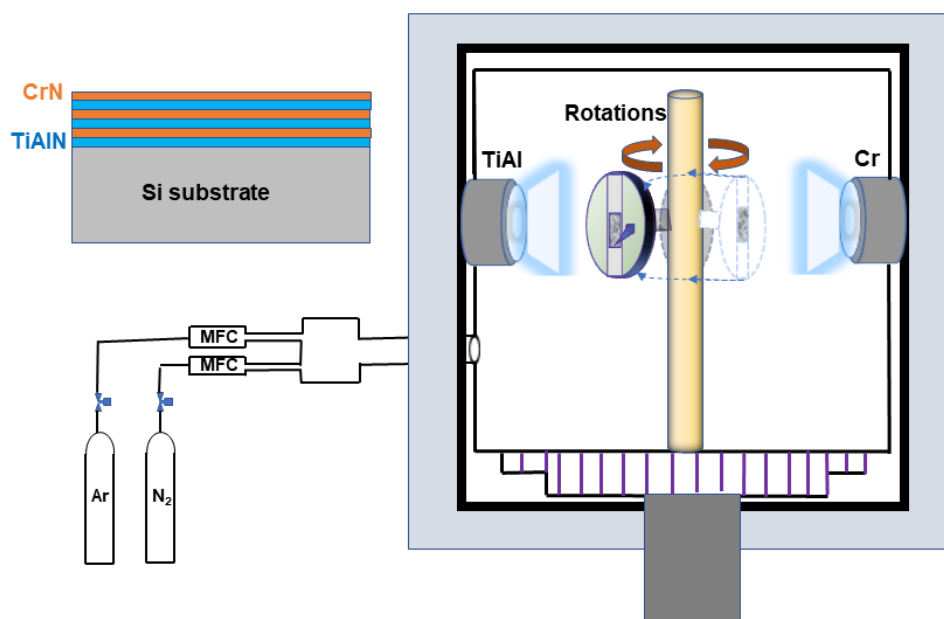


Fig. 1. Schematic illustration of sputter system with a rotating substrate holder

### 3. Results and discussion

#### 3.1. Structure analysis

The XRD patterns of TiAlN, CrN, and TiAlN/CrN multilayer coatings are shown in Fig. 2. All the samples showed good crystallinity with a cubic structure characterized by (200), (211), and (021) diffraction peaks. The lattice parameters of TiAlN and CrN were calculated using Bragg's law and the peak positions and were found to be  $a = 4.08 \text{ \AA}$  and  $4.12 \text{ \AA}$ , respectively, which are consistent with the previously reported values [15]. The TiAlN and CrN showed a high-intensity major peak in the (200) direction at the  $42^\circ$  and  $42.5^\circ$  peak positions. It was observed that substrate reflections from the detector caused some background peaks. The crystallite size was determined using the following equation [16]

$$D = \frac{K\lambda}{\beta \cos \theta}, K = 0.9 \quad (1)$$

where  $D$  is the crystallite size,  $k$  is the Scherrer constant,  $\beta$  is the full width at half maximum in radian,  $\lambda$  is the wavelength of the X-ray, and  $\theta$  is the Bragg's diffraction angle. The obtained values were in the range of 9.66–24.87 nm and 13.43–40.05 nm for TiAlN and CrN thin films, respectively. The Williamson-Hall method [17] can provide more accurate information about the microstructure of the material and calculated the crystallite size from the following equation

$$\beta_{hkl} \cos \theta_{hkl} = \frac{k\lambda}{D} + 4\varepsilon \sin \theta_{hkl} \quad (2)$$

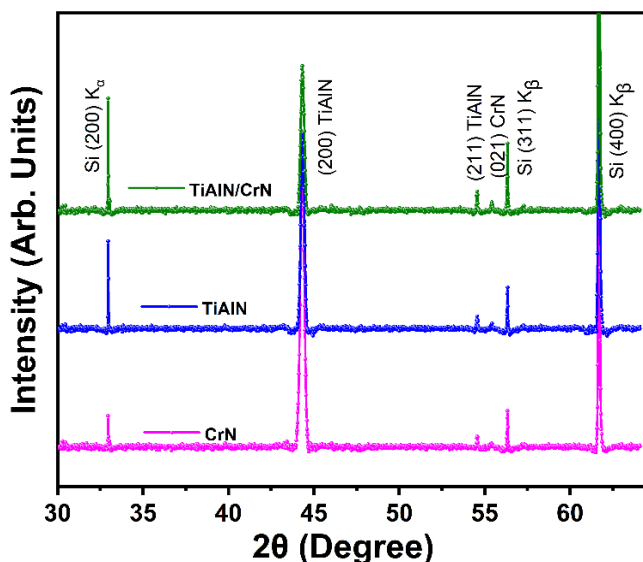


Fig. 2. XRD pattern for CrN, TiAlN, and TiAlN/CrN multilayer nano-composite thin films

The calculated structural parameters of the deposited thin films are listed in TABLE 1. The crystallite size and micro-strain were calculated as 25.12 nm and  $2.70 \times 10^{-2}$  for TiAlN, and 32.50 nm and  $2.10 \times 10^{-2}$  for CrN coatings. The relation-

ship between crystallite size and hardness is governed by the Hall-Petch effect [18], which states that the hardness of a material increases with decreasing grain size. As a result, the CrN coating exhibits a lower hardness than the TiAlN coating due to its larger grain size. The higher hardness of the TiAlN/CrN coating is likely due to a combination of factors, including its phase condition, the strength of its CrN orientations, and the compactness of the coating.

TABLE 1

Structural parameters of TiAlN and CrN thin films deposited at  $300^\circ\text{C}$  temperature

Parameters	TiAlN	CrN
Lattice parameters ( $\text{\AA}$ )	$a = b = c = 4.08$	$a = b = c = 4.12$
Debye-Scherrer method ( $D$ , nm)	9.66–24.87	13.43–40.05
Williamson-Hall method ( $D$ , nm)	25.12	32.50
Micro-strain	$2.70 \times 10^{-2}$	$2.10 \times 10^{-2}$
Dislocation density ( $1/D^2$ , $\text{nm}^{-2}$ )	$15.84 \times 10^{-4}$	$9.46 \times 10^{-4}$
Unit cell volume ( $V$ , $\text{\AA}^3$ )	67.91	69.93

The XRD of multilayer films had a higher degree of orientation than the single layer films, with the (200) peak being the strongest peak in both TiAlN and CrN layers. This suggests that the growth of the multilayer films was controlled by the orientation of the underlying layers, with the TiAlN and CrN layers preferentially growing in the (200) direction. The increased orientation of the multilayer films may contribute to their improved mechanical properties, as it allows for better distribution of stress and strain within the coating.

#### 3.2. Multilayer thin film cross-section analysis

HR-TEM analysis was performed on TiAlN/CrN multilayer thin films to investigate their multilayer structure. The resulting image, shown in Fig. 3a, reveals that the interface between the TiAlN and CrN layers is coherent and exhibiting the columnar grains starting from the TiAlN interlayer along the growth directions, which impacts the material's strength, toughness, and corrosion resistance [14]. A clear multilayer structure with symmetrical thickness was observed, with a total film thickness of  $\sim 20$  nm and individual layers of  $\sim 9.6$  nm TiAlN and  $\sim 11.2$  nm CrN. The CrN and TiAlN layers show minimal intermixing at the interface, indicating a well-defined boundary between them. The average bilayer thickness is 22 nm, and the modulation ratio is  $\sim 1:1$ .

The HAADF scanning transmission electron microscopy (STEM) image, with the elemental concentration profiling of the TiAlN/CrN multilayer thin film, is shown in Fig. 3b. The image reveals the chemical composition of the film, with the TiAlN layers appearing dark and the CrN layers appearing bright. This is due to the difference in atomic numbers between Cr and the other two elements, Ti and Al. Upon closure inspection reveals that the position of the Al and Ti concentration peaks are slightly

shifted with respect to each other. This shift indicates that slight decomposition of the TiAlN layers occurs during the deposition process. Fig. 3c presents an elemental color mapping of the multilayer coating, with Ti and Al represented by yellow and blue, respectively, and Cr and nitrogen represented by green and red. This image shows evidence of intermixing between the elements, likely due to the thinness of each layer (~10 nm).

### 3.3. Surface roughness analysis

The surface roughness and texture of coatings play a crucial role in determining their quality, including their adhesion, friction, cohesion, and wear properties. AFM was used to evaluate these properties of the deposited nanolayered coatings. Fig. 4(a-c) shows the AFM images of the deposited materials with a 200 nm scale scanned in the  $1 \times 1 \mu\text{m}^2$  scanned area. The TiAlN and CrN thin film surfaces show an island-like structure, corresponding to the grains. The TiAlN/CrN multilayer coating appears to be uniform and dense. The TiAlN film has an RMS roughness of 61.20 nm, the CrN film has an RMS roughness of 80.75 nm, and the TiAlN/CrN multilayer film has an RMS roughness of 29.06 nm. These results indicate that the TiAlN/CrN multilayer film has a much smoother surface compared to the single-layer TiAlN and CrN films. This could be because the TiAlN/CrN multilayer coatings create an intermediate buffer layer which prevents the growth of large grains and agglom-

erations. Furthermore, the TiAlN layer may help to inhibit the growth of dense and clustered grains, resulting in a smoother surface. This makes multilayer coatings a great choice for applications such as wear resistant coatings, corrosion protection, and heat/thermal management.

### 3.4. Mechanical properties

To determine the hardness and Young's modulus of the single and multilayered thin films, the deposited samples were characterized using Depth-sensing indentation measurements. The load was applied and then released or unloaded on the surface of the thin films at five different locations, and the resulting indentation was measured using a high-resolution microscope, as shown in Fig. 5(a-c). From Fig. 5, it was observed that the TiAlN coating scattered considerably compared to the CrN coating, while the TiAlN/CrN coating load-unload curves from different locations are almost overlapped. The hardness and elastic modulus of the thin films were then calculated from the indentation depth, size, applied load, and unloading conditions. This process was repeated at each of the five locations in order to obtain a representative measure of the hardness and elastic modulus of the thin films. Table 2 shows the mean and standard deviation of the hardness values for each of the three samples, using three different measurement techniques, indentation hardness ( $H_{IT}$ ), Vickers hardness ( $HV_{IT}$ ), and elastic indentation technique ( $E_{IT}$ ).

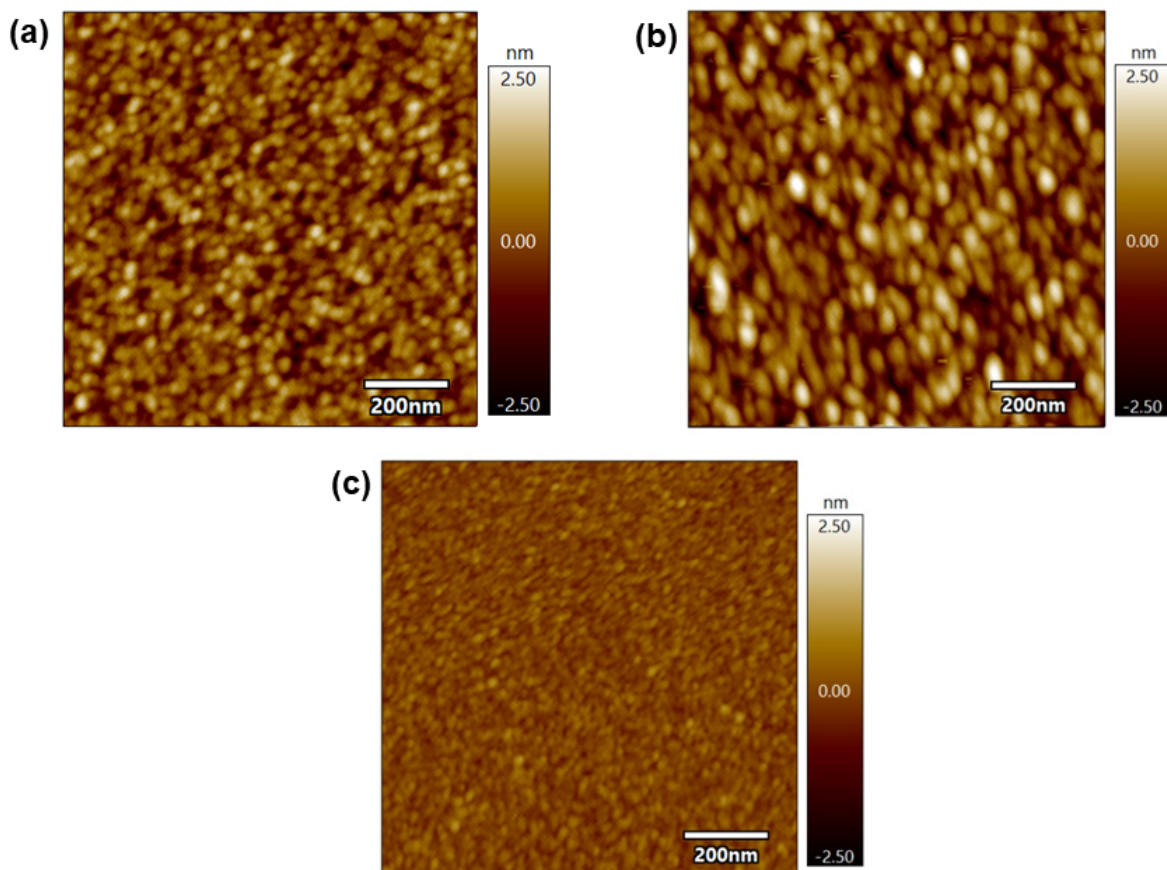


Fig. 4. Surface topography of (a) TiAlN (b) CrN (c) TiAlN/CrN multilayer thin films in the scan area of  $1 \times 1 \mu\text{m}^2$



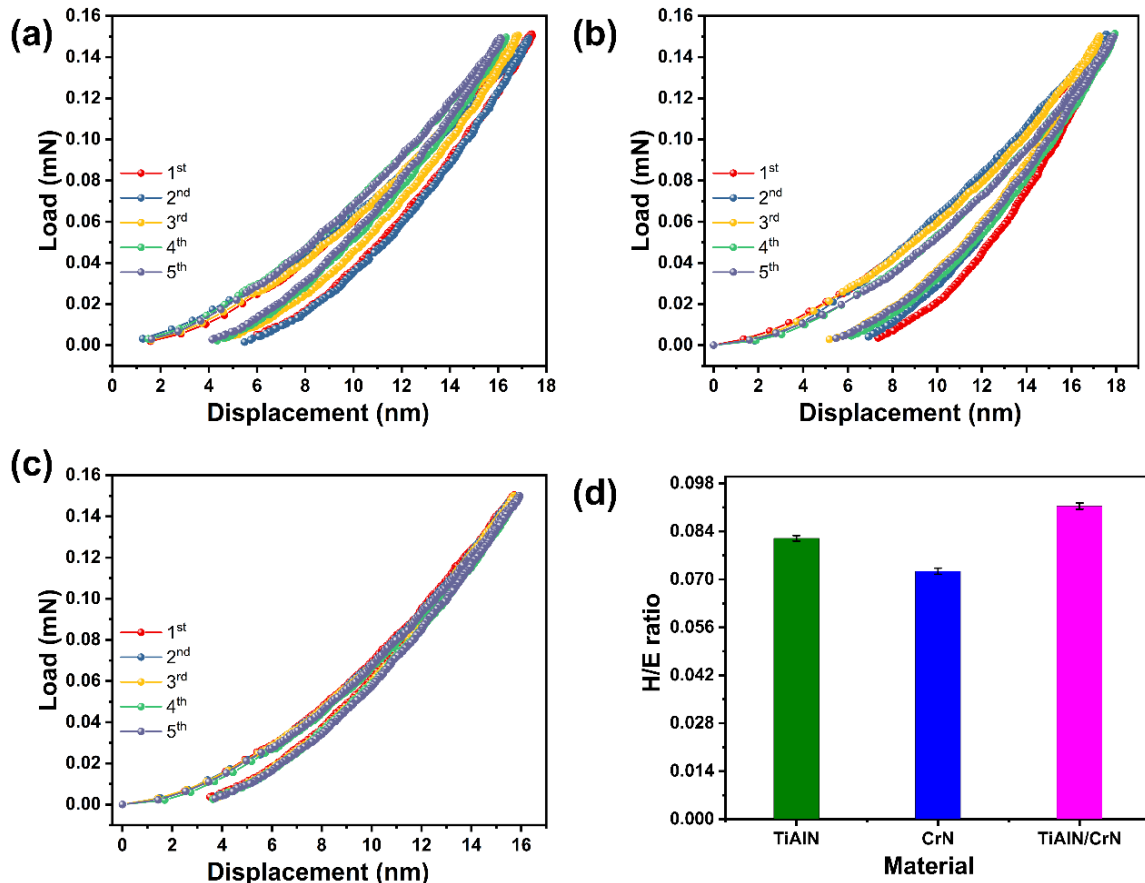


Fig. 5. Load-unload curves of (a) TiAlN (b) CrN (c) TiAlN/CrN thin films at five different locations (d) H/E ratio of TiAlN, CrN, and TiAlN/CrN thin films

The H/E ratio reflects the elastic strain to failure of a material [19] which is the amount of elastic deformation a material can undergo before it yields or permanently deforms. These properties can be useful in predicting the behavior of coatings in wear applications. According to Matthews and Leyland's theory, the higher H/E ratio denotes excellent wear resistance [20].

TABLE 2

Comparison of mechanical properties for TiAlN, CrN, and TiAlN/CrN coatings

		TiAlN	CrN	TiAlN/CrN
$H_{IT}$ (O&P)	Mean	13.747	11.921	16.282
	Std Dev	1.399	0.696	0.270
$HV_{IT}$ (O&P)	Mean	1273.177	1104.023	1507.950
	Std Dev	129.654	64.501	25.040
$E_{IT}$ (O&P)	Mean	167.596	164.671	178.132
	Std Dev	5.034	14.612	3.493

TABLE 2 presents the results of nanoindentation tests performed on TiAlN, CrN, and TiAlN/CrN coatings. The values for the TiAlN coating indicate that it has a higher hardness and indentation toughness compared to the CrN coating. The TiAlN/CrN coating has the highest values for all three properties, indicating that it has superior mechanical properties compared to

single-layer coatings. This is due to the strengthening effects of the interfacial layers in the multi-layer structure of the film. These interfacial layers can enhance the mechanical properties of the film through a combination of different strengthening mechanisms, such as the alternating stress field effect and Koehler's modulus-difference theory [21]. These mechanisms can increase the hardness and other mechanical properties of the film, making it more resistant to deformation and wear.

#### 4. Conclusions

In conclusion, the study showed that multilayer nanocomposite thin films, specifically TiAlN/CrN, have superior structural, morphological and mechanical properties compared to single-layered materials. The XRD, TEM, AFM, and nanoindentation results revealed that the multilayer film exhibited a coherent interface, with no intermixing of the TiAlN and CrN layers and a smoother surface. In addition, the multilayer structure created a buffer layer that prevented the growth of large grains and agglomerations, contributing to the higher hardness and elastic modulus values of the TiAlN/CrN multilayer coating. Overall, the TiAlN/CrN multilayer coating has excellent wear and corrosion resistance, making it a promising candidate for advanced machining applications.

### Acknowledgements

This research was supported by the research fund of Hanbat National University in 2020.

### REFERENCES

- [1] S. Kumar, S.R. Maity, L. Patnaik, Effect of annealing on structural, mechanical and tribological properties of Cr-(CrN/TiAlN) coating. *Adv. Mater. Process. Technol.* **8** (3), 1569-1582 (2021). DOI: <https://doi.org/10.1080/2374068x.2021.1946755>
- [2] H. Olia, R. Ebrahimi-Kahrizsangi, F. Ashrafizadeh, I. Ebrahimzadeh, Corrosion study of TiN, TiAlN and CrN multilayer coatings deposit on martensitic stainless steel by arc cathodic physical vapour deposition. *Mater. Res. Express* **6** (4), (2019). DOI: <https://doi.org/10.1088/2053-1591/aaff11>
- [3] P.E. Hovsepian, A.A. Sugumaran, M. Rainforth, J. Qi, I. Khan, A.P. Ehiasarian, Microstructure and load bearing capacity of TiN/NbN superlattice coatings deposited on medical grade CoCrMo alloy by HIPIMS. *J. Mech. Behav. Biomed. Mater.* **132**, 105267 (2022). DOI: <https://doi.org/10.1016/j.jmbbm.2022.105267>
- [4] J. Caicedo, N. Bonilla, W. Aperador, Corrosion Nature in [CoN/AlN]<sub>n</sub> Multilayers Obtained from Laser Ablation. *Metals* **11** (12), (2021). DOI: <https://doi.org/10.3390/met11122049>
- [5] L. Wang, M. Wang, H. Chen, Corrosion mechanism investigation of TiAlN/CrN superlattice coating by multi-arc ion plating in 3.5 wt% NaCl solution. *Surf. Coat. Technol.* **391**, (2020). DOI: <https://doi.org/10.1016/j.surfcoat.2020.125660>
- [6] C.-L. Chang, C.-H. Huang, C.-Y. Lin, F.-C. Yang, J.-F. Tang, Mechanical properties of amorphous and crystalline CrN/CrAlSiN multilayer coating fabricated using HPPMS. *Surf. Interfaces* **31**, (2022). DOI: <https://doi.org/10.1016/j.surfin.2022.102064>
- [7] A. Thakur, S. Gangopadhyay, Dry machining of nickel-based super alloy as a sustainable alternative using TiN/TiAlN coated tool. *J. Cleaner Prod.* **129**, 256-268 (2016). DOI: <https://doi.org/10.1016/j.jclepro.2016.04.074>
- [8] A.I. Kovalev, Impact of Al and Cr alloying in TiN-based PVD coatings on cutting performance during machining of hard to cut materials. *Vacuum* **84** (1), 184-187 (2009). DOI: <https://doi.org/10.1016/j.vacuum.2009.06.019>
- [9] Y.X. Xu, L. Chen, F. Pei, Y. Du, Structure and thermal properties of TiAlN/CrN multilayered coatings with various modulation ratios. *Surf. Coat. Technol.* **304**, 512-518 (2016). DOI: <https://doi.org/10.1016/j.surfcoat.2016.07.055>
- [10] H.C. Barshilia, B. Deepthi, K.S. Rajam, K.P. Bhatti, S. Chaudhary, Growth and characterization of TiAlN/CrAlN superlattices prepared by reactive direct current magnetron sputtering. *J. Vac. Sci. Technol. A* **27** (1), 29-36 (2009). DOI: <https://doi.org/10.1116/1.3013858>
- [11] B. Liu, B. Deng, Y. Tao, Influence of niobium ion implantation on the microstructure, mechanical and tribological properties of TiAlN/CrN nano-multilayer coatings. *Surf. Coat. Technol.* **240**, 405-412 (2014). DOI: <https://doi.org/10.1016/j.surfcoat.2013.12.065>
- [12] B. Warcholinski, A. Gilewicz, Mechanical properties of multilayer TiAlN/CrN coatings deposited by cathodic arc evaporation. *Surf. Eng.* **27** (7), 491-497 (2013). DOI: <https://doi.org/10.1179/026708410x12786785573355>
- [13] R.N. Ibrahim, M.A. Rahmat, R.H. Oskouei, R.K. Singh Raman, Monolayer TiAlN and multilayer TiAlN/CrN PVD coatings as surface modifiers to mitigate fretting fatigue of AISI P20 steel. *Eng. Fract. Mech.* **137**, 64-78 (2015). DOI: <https://doi.org/10.1016/j.engfracmech.2015.01.009>
- [14] M. Panjan, S. Šturm, P. Panjan, M. Čekada, TEM investigation of TiAlN/CrN multilayer coatings prepared by magnetron sputtering. *Surf. Coat. Technol.* **202** (4-7), 815-819 (2007). DOI: <https://doi.org/10.1016/j.surfcoat.2007.05.084>
- [15] I. Povstugar, P.-P. Choi, D. Tytko, J.-P. Ahn, D. Raabe, Interface-directed spinodal decomposition in TiAlN/CrN multilayer hard coatings studied by atom probe tomography. *Acta Mater.* **61** (20), 7534-7542 (2013). DOI: <https://doi.org/10.1016/j.actamat.2013.08.028>
- [16] U. Holzwarth, N. Gibson, The Scherrer equation versus the 'Debye-Scherrer equation'. *Nat. Nanotechnol.* **6** (9), 534 (2011). DOI: <https://doi.org/10.1038/nnano.2011.145>
- [17] P. Bindu, S. Thomas, Estimation of lattice strain in ZnO nanoparticles: X-ray peak profile analysis. *J. Theor. Appl. Phys.* **8** (4), 123-134 (2014). DOI: <https://doi.org/10.1007/s40094-014-0141-9>
- [18] E.O. Hall, The Deformation and Ageing of Mild Steel: III Discussion of Results. *Proc. Phys. Soc. B* **64**, 747 (1951).
- [19] N.A. Sakharova, J.V. Fernandes, M.C. Oliveira, et al. Influence of ductile interlayers on mechanical behaviour of hard coatings under depth-sensing indentation: a numerical study on TiAlN. *J. Mater. Sci.* **45**, 3812-3823 (2010). DOI: <https://doi.org/10.1007/s10853-010-4436-1>
- [20] M.C. Joseph, C. Tsotsos, M.A. Baker, P.J. Kench, C. Rebholz, A. Matthews, A. Leyland, Characterisation and tribological evaluation of nitrogen-containing molybdenum-copper PVD metallic nanocomposite films. *Surf. Coat. Technol.* **190**, 345-356 (2005). DOI: <https://doi.org/10.1016/j.surfcoat.2004.04.074>
- [21] X. Gu, Z. Zhang, M. Bartosik, P.H. Mayrhofer, H. Duan, Dislocation densities and alternating strain fields in CrN/AlN nanolayers. *Thin Solid Films* **638**, 189-200 (2017). DOI: <https://doi.org/10.1016/j.tsf.2017.07.042>
- [22] B. Gao, X.Y. Du, Y.H. Li, S.H. Wei, X.D. Zhu, Z.X. Song, Effect of deposition temperature on hydrophobic CrN/AlTiN nanolaminate composites deposited by Multi-Arc-Ion Plating. *J. Alloys Compd.* **797**, 1-9 (2019). DOI: <https://doi.org/10.1016/j.jallcom.2019.05.069>